

# Analytical Model of Asynchronous Shared-per-Wavelength Multi-fiber Optical Switch

Nail Akar

Electrical and Electronics Engineering Dept.  
Bilkent University, Ankara, Turkey  
email:akar@ee.bilkent.edu.tr

Carla Raffaelli

DEIS - University of Bologna  
Bologna, Italy.  
email:carla.raffaelli@unibo.it

Michele Savi

Department of Telematics - NTNU  
Trondheim, Norway.  
email:michele.savi@item.ntnu.no

**Abstract**— In this paper, a buffer-less shared-per-wavelength optical switch is equipped with multi-fiber interfaces and operated in asynchronous context. An analytical model to evaluate loss performance is proposed using an approximate Markov-chain based approach and the model is validated by simulations. The model is demonstrated to be quite accurate in spite of the difficulty in capturing correlation effects especially for small switch sizes. The model is also applied to calculate the number of optical components needed to design the optical switch according to packet loss requirements. The impact of the adoption of multiple fiber interfaces is outlined in terms of the remarkable saving in the number of wavelength converters employed, while increasing at the same time the number of optical gates needed by the space switching subsystem. The numerical results produced are a valuable basis to optimize overall switch cost.

## I. INTRODUCTION

Design and implementation of photonic packet switches have recently been considered as fundamental steps for the deployment of future Internet-based services [1],[2]. In recent years, optical technology is entering a quite mature phase which attracts increased attention to support the ever growing bandwidth-demanding needs of networking applications [3]. Therefore, a renewed interest in optical switching stimulates substantial amount of research to employ newly available optical components with enhanced reconfiguration capability. This is the case of switching components, like MEMS, SOAs, microring resonators, etc., and wavelength shifting components such as tuneable wavelength converters. In spite of the progress in optical technology fabrication, all optical wavelength converters are still considered complex components [3].

Wavelength converters are employed in dynamic optical switching to exploit the wavelength domain with the purpose of contention resolution. As a matter of fact, when two or more information units (or packets) need the same forwarding resource (optical gate, fiber interface, splitter/combiner) within the node, two different wavelengths are used to encode them, possibly by wavelength converting the related optical signal [4]. The quantity and type of wavelength converters employed to obtain a given logical performance has been demonstrated to be related to the specific switch architecture [5]. In particular, wavelength converters differ

on the basis of their tuneability and wavelength conversion range. It can be assessed that fixed wavelength converters are simpler to be fabricated with respect to tunable ones [6].

Previous studies introduced the shared-per-input-wavelength optical switching architecture [7] which employs fixed-input/tuneable-output wavelength converters. This architecture has been demonstrated to have superior properties regarding its feasibility [8], power consumption [9] and costs [10], while performing quite close to the shared-per-node architecture [5], [10].

The conversion range required by the wavelength converters is related to the number of wavelength channels supported by each fiber interface. The adoption of multi-fiber interfaces allows to repeat the same wavelength as many times as the number of fibers allocated at each interface, being them spatially separated. This solution has been studied for shared-per-node and shared-per-input-wavelength architectures in synchronous contexts [10]. Only the multi-fiber shared-per-node solution has been studied with asynchronous operation [11]. The interest for studying multi-fiber shared-per-input-wavelength architecture with asynchronous operation comes from the interesting properties of this architecture in terms of feasibility and power consumption, together with the possibility to limit the conversion range assured by multi-fiber interfaces, without the need of complex synchronizers as in slotted operation [12].

Based on previous motivations, in this paper a multi-fiber switch architecture with asynchronous operation which shares fixed-input wavelength converters is investigated to analytically obtain its logical performance in terms of packet loss probability. The architecture is named A-MF-SPIW (Asynchronous Multi-fiber Shared-Per-Input-Wavelength). To the best of our knowledge, such a study has not been in performed in the existing literature.

The paper is organized as follows. Sec. II describes the A-MF-SPIW architecture, its complexity and forwarding procedure. Sec. III presents the analytical model to evaluate packet loss. Sec. IV discusses model validation and some complexity evaluations related to the number of fibers per interface. Sec. V gives some conclusions of this work.

## II. THE A-MF-SPIW ARCHITECTURE

This section introduces the A-MF-SPIW architecture (Fig. 1) considering  $N$  input/output interfaces (II/OIs), each provided with  $F$  optical fibers carrying  $M$  wavelengths. The

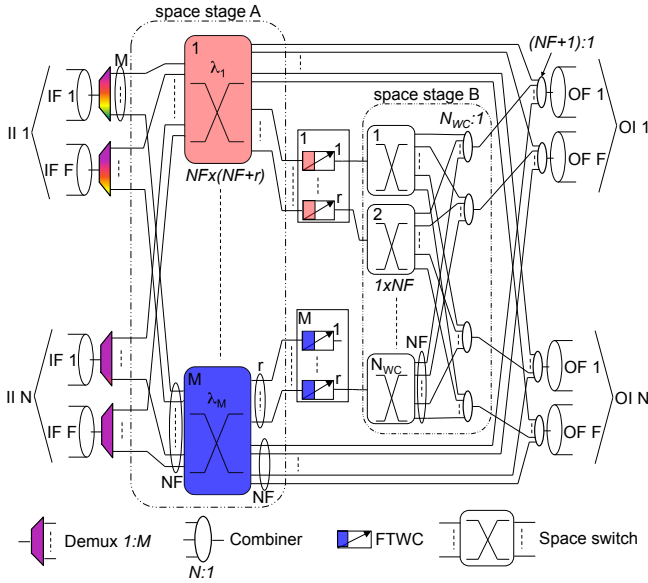


Fig. 1. A-MF-SPIW architecture with  $N$  input/output interfaces equipped with  $F$  optical fibers carrying  $M$  wavelengths each. The switch is equipped with  $M$  pools of  $r < NF$  WCs dedicated per input wavelength.

total number of channels per interface is  $N_C = MF$ . To solve contention in wavelength domain, the architecture is equipped with *fixed-input/tunable-output* Wavelength Converters (WCs) which are simpler and less expensive than *tunable-input/tunable-output* ones [6],[10]. WCs are partitioned in  $M$  pools of  $r < NF$  WCs each; each pool serves packets coming on the same wavelength, so WCs are shared-per-input-wavelength [7]. The total number of WCs is  $N_{WC} = Mr$  and their output range is  $M$ .

The architecture presented in Fig. 1 is now described in detail. In this architecture single-stage space switches are considered to connect IIs, OIs and WC pools. The architecture is organized to minimize the complexity in terms of Optical Gates (OGs) using such single-stage switches. OGs can be implemented for example by using Semiconductor Optical Amplifiers (SOAs), microring resonators, acousto-optical devices and so on. After wavelength demultiplexing, channels related to the same wavelength on the different input fibers ( $NF$ ) are connected to a space switch dedicated to that wavelength. The input fibers are connected to the space switches according to a shuffle permutation. Packets arriving at a space switch can be either directly forwarded to one of the  $NF$  output fibers or forwarded to the corresponding pool of  $r$  WCs. In this first *space stage A*, there are  $M$  space switches of size  $NF \times (NF+r)$ . After the WC stage, each WC is connected to a  $1 \times NF$  space switch needed to connect it to the proper output fiber. In

this *space stage B*, there are  $N_{WC} = Mr$  space switches. A set of  $NF$  combiners  $N_{WC} : 1$ , each connected to one of the output fibers, is used to multiplex the signals coming from the  $N_{WC}$  WCs. The  $N_{WC}$  space switches and the  $NF$  combiners are interconnected according to a shuffle permutation, so that each WC is connected to all combiners, and vice-versa. Finally, at the output fibers  $NF$  combiners  $(NF+1) : 1$  are used to multiplex the signals coming from the input fibers (up to  $NF$ ) and the signals coming from the WC pools. Neglecting the signals coming from the WCs, the signals from the input fibers are connected to the combiners according to a shuffle permutation.

The proposed architecture is equipped with multi-fiber interfaces; this kind of architecture is able to forward up to  $F$  packets coming on the same wavelength to the same OI (one packet per fiber), thus partially solving contention among packets on the same wavelength. In the single-fiber case ( $F = 1$ ), instead, only one packet per wavelength can be forwarded to the same OI. Assuming the number of channels per interface  $N_C = MF$  as a constant value, the higher the number of fibers per interface (denoted by  $F$ ), the better the packet loss performance even with no wavelength conversion. Furthermore, when wavelength conversion is considered, increasing  $F$  allows to reduce the number of WCs needed in the architecture (contention partially solved by multi-fiber solution) and also to reduce the range of each WC ( $MF$  constant, if  $F$  increases  $M$  decreases). This aspect will be further evidenced in Sec. IV.

On the other hand, increasing the number of fibers means also increasing the complexity of the architecture in terms of optical devices. So the best trade-off should be found to obtain desired performance with minimum complexity.

The complexity of the A-MF-SPIW architecture can be evaluated taking into account that the space stage A needs  $M$  single-stage space switches of size  $NF \times (NF+r)$  while the space stage B needs  $N_{WC}$  single-stage space switches of size  $1 \times NF$ . After some math (remembering that  $N_C = MF$  and  $N_{WC} = Mr$ ) the complexity can be expressed as

$$N_{OG} = N^2 F N_C + 2 N F N_{WC}. \quad (1)$$

Considering the first term, the complexity increases linearly with  $F$ . In the second term, the complexity increases linearly with  $F$  if the total number of WCs  $N_{WC}$  is fixed. It is anyway important to emphasize that  $N_{WC}$  decreases as  $F$  increases (see Sec. IV), so the dependence of the second term on  $F$  needs to be carefully evaluated.

A qualitative analysis of the complexity can be described as follows: in the space stage A, the size of each space switch increases as  $(NF)^2 + NF r = F^2 (N^2 + \frac{N}{N_C} N_{WC})$ , but the number of space switches ( $M = \frac{N_C}{F}$ ) is in inverse relation with  $F$ . In the space stage B, the size of each space switch increases as  $NF$ , and the number of space switches is related to  $N_{WC}$ , which decreases as  $F$  increases.

The architecture is operated in an asynchronous scenario, where a packet is scheduled as it arrives at the input

interface. When a packet arrives at the switch on wavelength  $w$ , the scheduling algorithm randomly selects one fiber (say  $f$ ) on the destination interface for which wavelength  $w$  is available and then the packet is forwarded to wavelength  $w$  of fiber  $f$ . If all the wavelength channels related to  $w$  are busy on the destination interface then the outgoing wavelength (say  $g$ ) is selected randomly among the ones that are free on at least one fiber of the destination interface. One of such output fibers (say  $h$ ) is randomly selected and the packet is forwarded on wavelength  $g$  of fiber  $h$  using one of the WCs in the pool dedicated to the incoming wavelength  $w$ . A packet is lost either when all  $N_C$  channels on the destination interface are busy at the time the packet arrives or when the arriving packet requires conversion and all  $r$  WCs dedicated to wavelength  $w$  are busy. More complex scheduling policies are left for future research. The analytical model presented in Sec. III is developed taking the scheduling procedure described above into account.

### III. ANALYTICAL MODEL OF A-MF-SPW

In the proposed model, the traffic destined to OI  $n$  ( $n = 1, \dots, N$ ), is assumed to be a Poisson process with intensity  $\lambda$ . The total packet arrival rate to the switch is then  $N\lambda$ . We also assume that the wavelength of an incoming optical packet is assumed to be uniformly distributed over the  $M$  wavelengths. Packet lengths are assumed to be exponentially distributed with mean set to unity and therefore the time unit in this article is set to the mean packet length. More general traffic patterns in which different OIs receive different intensities of traffic are left for future research. The load per input channel is denoted by  $p = \frac{\lambda}{MF} = \frac{\lambda}{N_C}$ .

Let us now focus on a tagged OI  $n$  whose statistical nature is the same as the other OIs. Let  $L(t)$  denote the number of occupied wavelength channels for OI  $n$  at time  $t$ . The process  $L(t) \in \{0, 1, \dots, N_C\}$  is not a Markov process but under some assumptions (which will be clarified later on), it can be approximated by a Markov process. For this purpose, we have the following two assumptions:

- When  $L(t) = i$ , the probability that an arriving packet requires conversion is  $p_i$  ( $i = 0, 1, \dots, N_C - 1$ ).
- Given that a packet requires conversion, the probability of this packet to find all converters busy in its associated pool is given by  $p_B$  and this probability is independent from the process  $L(t)$ .

Under these two assumptions, the random process  $L(t)$  can be shown to be a non-homogeneous birth-death (BD) type Markov chain. The birth rate  $\eta_i$  of this chain at state  $i$  (the transition rate from state  $i$  to  $i + 1$ ) is then given by

$$\eta_i = \lambda(1 - p_i) + \lambda p_i(1 - p_B), i = 0, \dots, N_C - 1, \quad (2)$$

The death rate at state  $i$  is denoted by  $\mu_i = i$  (transition rate from state  $i$  to  $i - 1$ ) due to exponential packet lengths with parameter one. If the probabilities  $p_i$  and  $p_B$  were known, then we could find the steady-state probabilities  $\pi_i$  ( $i = 0, 1, \dots, N_C$ ) of this Markov chain which actually is the

steady-state probability that the Markov chain corresponding to OI  $n$  is visiting state  $i$ . Because of the ‘‘Poisson arrivals see time averages’’ property the packet loss probability (PLP) for a packet directed to OI  $n$  can be expressed as

$$PLP = \pi_{N_C} + \sum_{i=1}^{N_C-1} \pi_i p_i p_B, \quad (3)$$

The first term amounts to the case when an arriving packet finds all  $N_C$  wavelength channels occupied. On the other hand, the second term considers the case when there are idle channels on the OI but the packet requires conversion and is dropped due to the lack of a suitable WC.

However, the quantities  $p_B$  and  $p_i$  are not known yet. For the former quantity, the intensity of the traffic destined to OI  $n$  requiring conversion is given by

$$\nu = \sum_{i=1}^{N_C-1} \lambda \pi_i p_i. \quad (4)$$

The intensity of the overall traffic destined to the WC pool dedicated to a particular wavelength  $w$  is  $\frac{N\nu}{M}$ . There are indeed  $N$  OIs and the overall traffic is uniformly distributed among  $M$  WC pools. Under the assumption that this traffic is Poisson, the quantity  $p_B$  can be obtained using the Erlang-B formula corresponding to the case of  $r$  servers fed with Poisson traffic with utilization  $\frac{N\nu}{M}$ .

Next, we describe how we approximate the quantity  $p_i$  for  $i = 1, \dots, N_C - 1$ . For the purpose of approximating the quantity  $p_i$ , we first assume no wavelength conversion, i.e.,  $r = 0$ . In this case for the designated OI  $n$  we have  $M$  server groups each one with  $F$  servers and fed with Poisson traffic with intensity  $\frac{\lambda}{M}$ . Due to the lack of WCs, server groups are independent from each other and the steady-state occupancy probabilities of each server group can be found from the M/M/F/F queue formalism. Let  $x_j$  denote the steady-state probability of  $j$  channels being occupied for OI  $n$  when  $r = 0$ . Note that the probabilities  $x_j$ s can be found on the basis of the steady-state distribution of an individual M/M/F/F queue but a detailed description of their efficient calculation is omitted in this paper due to space limitations. Now, consider the following birth-death process  $X(t)$  with death rate at state  $j$   $\mu_j = j$  and birth rate  $\beta_j$

$$\beta_j = \frac{x_{j+1}\mu_{j+1}}{x_j} = \frac{x_{j+1}(j+1)}{x_j}, j = 0, 1, \dots, N_C - 1. \quad (5)$$

It is clear from the global balance equations of this Markov chain that  $x_j$  is the steady-state probability  $\lim_{t \rightarrow \infty} P(X(t) = j)$ . When  $r = 0$ , although a one-dimensional Markov chain does not suffice to represent the system behavior, the one-dimensional Markov chain constructed above using  $x_j$  has the correct steady-state probabilities  $x_j$  and therefore can be used to approximate system behavior when  $r = 0$ . We propose in this article to choose  $p_i$  such that the birth rates of the two Markov chains corresponding to  $L(t)$  and  $X(t)$  are the same when  $r = 0$

and thus  $p_B = 1$ . By comparing (2) and (5) with  $p_B = 1$  we can write  $\lambda(1 - p_i) = \beta_i$  or equivalently

$$p_i = 1 - \frac{\beta_i}{\lambda}, i = 0, 1, \dots, N_C - 1. \quad (6)$$

We have shown that choosing  $p_i$  in this way allows one to use a one-dimensional Markov chain  $L(t)$  or  $X(t)$  to correctly find the loss probabilities for the case  $r = 0$ .

For the case  $r > 0$ , it is worth noting that the probability that a packet requires wavelength conversion is independent from the number of WCs available and the particular sharing scheme adopted which indeed only affects the packet loss due to lack of WC ( $p_B$ ). So the conversion probabilities  $p_i$  should not be sensitive to the particular value of  $r$  and they can be maintained also in the case  $r > 0$ . To summarize the whole fixed-point procedure, an arbitrary  $p_B$  is first considered to construct the Markov chain  $L(t)$  using  $p_i$ s as given in (6). The Markov chain is then solved to find probabilities  $\pi_i$  and the probability  $p_B$  is re-calculated for an  $r$ -server system fed with Poisson traffic with intensity  $N\nu/M$  where  $\nu$  is defined as in (4). This procedure is then repeated until convergence, i.e. until two successive values for  $p_B$  are as close to each other as desired. Finally (after convergence) the expression (3) is used to evaluate PLP.

#### IV. NUMERICAL RESULTS

This section presents model validation and a set of results related to PLP and complexity of the A-MF-SPIW switch. To validate the analytical model, analysis is compared against simulation results obtained by applying the random scheduling procedure described in Sec. II to Poisson arrivals. Simulation results have been obtained with confidence interval equal to or less than 10% of the average loss, with 95% probability. To make the relationship between the loss probability and the number of WCs clear in the figures, the conversion ratio  $\alpha = \frac{N_{WC}}{NN_C} = \frac{r}{NF}$  is here introduced.  $\alpha$  normalizes the total number of WCs with respect to its maximum value  $NN_C$ . The range of values for  $\alpha$  is between 0 (no conversion case) and 1 (one WC per input channel). It is worthwhile noting that only some discrete values are allowed for  $\alpha$ , indeed every time a WC per wavelength is added,  $r$  increase of 1 unit, while  $N_{WC}$  increases of  $M$ .

Figure 2 depicts the PLP as a function of the conversion ratio  $\alpha$ , for analysis (A) and simulation (S) for the case  $N = 16$ ,  $N_C = MF = 16$  and  $p = 0.3$ . The number of fibers per interface varies as  $F = 1, 2, 4, 8$  and the parameter  $M$  changes accordingly. The figure shows how analytical results perform close to the simulation, even if the model underestimates PLP. The model captures the trend of the curves in the region where the number of WCs is limited, which is not trivial in the multi-fiber case. The model also perfectly captures the asymptotic value of PLP, which is related to the loss due to output blocking on the output fibers and only depends (under the same load condition) on the total number of channels  $N_C$  (kept

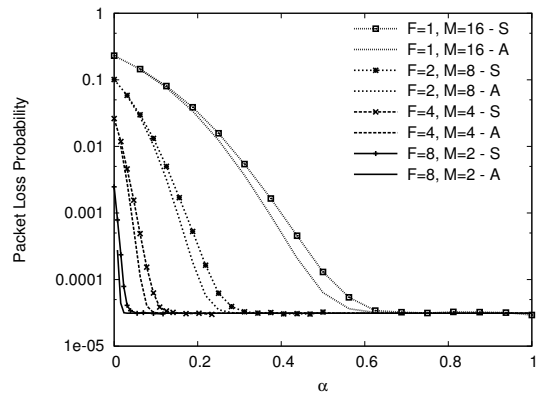


Fig. 2. PLP as a function of the conversion ratio  $\alpha$  for analysis (A) and simulation (S). PLP is shown as in the case  $N = 16$ ,  $N_C = MF = 16$ ,  $p = 0.3$  and  $F$  varying from 1 to 8.

constant here). As a matter of fact, PLP modeling when  $F$  increases is a non-trivial problem due to the correlations among packets, especially in the current case where WCs are partitioned among the wavelengths. The proposed model maintains an adequate level of accuracy for all values of  $F$  allowing to identify the number  $\alpha_{th}$  of WCs needed to reach asymptotic performance. The figure shows that  $\alpha_{th}$  rapidly decreases when  $F$  increases, due to the reuse of wavelengths in different fibers as explained in II.

Having verified that the model produces good results even for high  $F$ , the effect of other parameters ( $p$ ,  $N_C$ ,  $N$ ) on the accuracy of the model will now be evaluated. Fig. 3 depicts the PLP as a function of  $\alpha$ , for the case  $N = 16$ ,  $F = 2$ ,  $M = 8$ , and varying the load as  $p = 0.2, 0.3, 0.5, 0.7$ . The

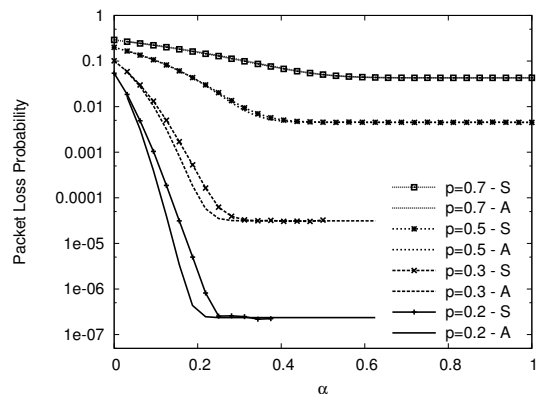


Fig. 3. PLP as a function of the conversion ratio  $\alpha$  for analysis (A) and simulation (S). PLP is shown as in the case  $N = 16$ ,  $N_C = MF = 16$  ( $F = 2$ ,  $M = 8$ ) varying load ( $p = 0.2, 0.3, 0.5, 0.7$ ).

accuracy of the model is very good when the load is high, due to the high loss related to blocking, which shadows the approximation introduced in the evaluation of the loss on WC pools. When the load decreases, the underestimation provided by the model increases, even if the minimum number of WCs needed for asymptotic performance can be

evaluated using the model with good accuracy (recall that  $\alpha$  is a discrete value). This trend as a function of load is present in all switch configurations.

Fig. 4 presents further comparison between analysis and simulations by varying  $N_C$  but with fixed  $N$ , for the scenario  $N = 16$ ,  $N_C = 16, 32$  and  $p = 0.4$ . In particular, the cases  $(F = 1, M = 16)$ ,  $(F = 4, M = 4)$  and  $(F = 1, M = 32)$ ,  $(F = 4, M = 8)$  are considered for  $N_C = 16$  and  $N_C = 32$ , respectively. The model provides results closer to the

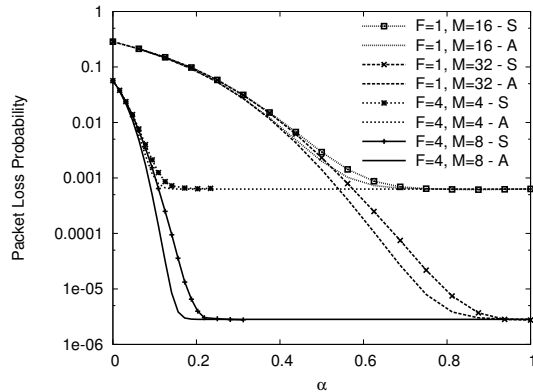


Fig. 4. PLP as a function of  $\alpha$  for analysis (A) and simulation (S). PLP is shown as in the case  $N = 16$ ,  $N_C = 16, 32$  and  $p = 0.4$ . The cases  $(F = 1, M = 16)$ ,  $(F = 4, M = 4)$  and  $(F = 1, M = 32)$ ,  $(F = 4, M = 8)$  are considered for  $N_C = 16$ ,  $N_C = 32$ , respectively.

simulation when  $N_C$  is lower, due to the higher asymptotic PLP (same effect as explained for previous figure). The discrepancy between analysis and simulation is in the same order of the one obtained in Fig. 2, in fact the asymptotic losses obtained in these cases are comparable. By observing Fig. 4, it is possible to extract peculiar information. For example when  $N_C$  increases the PLP rapidly decreases due to statistical multiplexing gain. When the number of WCs is limited, PLP obtained with  $N_C = 16$ ,  $N_C = 32$  is the same. This is due to the fact that in this case the loss in the WC pools dominates the overall loss; given that WCs are partitioned among the wavelengths, this loss is only related to the number of channels on the same wavelength, which is  $NF$  (see Fig. 1). As a matter of fact, there are the same number  $NF$  of input channels competing on the same wavelength when  $(F = 1, M = 16)$ ,  $(F = 1, M = 32)$  and when  $(F = 4, M = 4)$ ,  $(F = 4, M = 8)$ . Only when the number of WCs increases enough, and the loss in the WC pools becomes negligible, the PLP moves to different asymptotic values, related to  $N_C$ .

A final comparison varying  $N$  with fixed  $N_C$  is presented in Fig. 5. The PLP is plotted for  $N = 8$  and  $N = 20$ , considering  $N_C = 24$  and in particular the cases  $(F = 1, M = 24)$ ,  $(F = 4, M = 6)$ . The figure highlights how the model is less precise when  $N$  is small, for both values of  $F$ . The model approximation is acceptable for  $N = 20$ , while for  $N = 8$  the gap between analysis and simulation is notable.

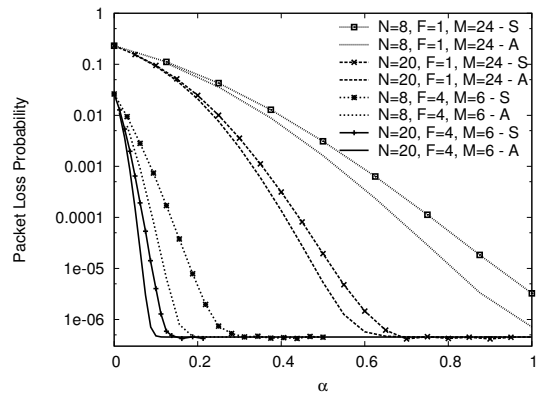


Fig. 5. PLP as a function of the conversion ratio  $\alpha$  for analysis (A) and simulation (S). PLP is shown as in the case  $N = 8, 20$ ,  $N_C = 24$ ,  $p = 0.3$ . For both  $N = 8$  and  $N = 20$  two cases are considered:  $(F = 1, M = 24)$ ,  $(F = 4, M = 6)$ .

This is due to the fact that for small  $N$ , individual fibers and WC pools become very correlated which is ignored in our analytical model. Therefore,  $N$  needs to be relatively large, i.e.,  $N \geq 8$ , for such fixed-point approximations to hold and provide good results and accuracy is increased with increasing number of interfaces. Note that also the performance of the A-MF-SPIW switch improves for large  $N$ , as can be deduced from previous figure, due to the better sharing of WC pools with high  $N$ . Thus, the model performs better exactly in such configurations where the proposed architecture gives best performance.

To provide an example of switch dimensioning, Fig. 6 shows the total number of WCs needed to obtain the PLP lower than a certain value ( $1e-3$ ,  $1e-4$ ,  $1e-5$ ,  $1e-6$ ) as a function of  $F$ , as in the case  $N = 20$ ,  $N_C = 24$ ,  $p = 0.3$ . This value is indicated with  $N_{WC}^{th}$ . Fig. 6 can be obtained

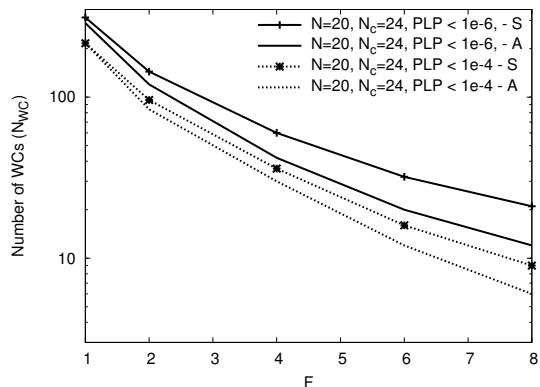


Fig. 6. Total number of WCs  $N_{WC}^{th}$  needed to obtain PLP lower than a certain value ( $1e-4$ ,  $1e-6$ ) as a function of  $F$ , as in the case  $N = 20$ ,  $N_C = 24$ ,  $p = 0.3$ . (A) stands for analysis and (S) for simulation.

by using Fig. 5 and similar and by taking into account that  $N_{WC} = \alpha N N_C$ . The figure shows values obtained using both analysis and simulation.  $N_{WC}^{th}$  rapidly decreases as

$F$  increases, for both values of PLP. The error in switch dimensioning using analysis is quantified by the figure and it increases as  $F$  increase, due to the fact that with high  $F$  PLP rapidly decreases in the region where  $N_{WC}$  is low (see Fig. 5). The figure gives an idea about the relative error with respect to the total number of WCs, which is low when  $F$  is low, and then increases almost linearly. The model provides good estimation of  $N_{WC}^{th}$  when  $F$  is not very high, which seems to be a reasonable trade-off in terms of complexity.

Evaluation of switch complexity is provided in Tables I and II, which contain the values of  $\alpha^{th}$ ,  $N_{WC}^{th}$  and  $N_{OG}$  needed to obtain  $PLP \leq 1e-4$  and  $1e-6$ , respectively, as in the case  $N = 20$ ,  $N_C = 24$ ,  $p = 0.3$ . The number of WCs  $N_{WC}^{th}$  is obtained from previous figure while OGs  $N_{OG}$  is obtained by applying formula (1), accordingly. Tables show values for different couples ( $F$ ,  $M$ ) while keeping the total number of channel as a constant,  $N_C = 24$ . The tables show

		$(F, M)$				
		(1, 24)	(2, 12)	(4, 6)	(6, 4)	(8, 3)
A	$\alpha^{th}$	0.45	0.175	0.0625	0.025	0.0125
	$N_{WC}^{th}$	216	84	30	12	6
	$N_{OG}$	18240	25920	43200	60480	78720
S	$\alpha^{th}$	0.45	0.2	0.075	0.03333	0.01875
	$N_{WC}^{th}$	216	96	36	16	9
	$N_{OG}$	18240	26880	44160	61440	79680

TABLE I

VALUES OF  $\alpha^{th}$ ,  $N_{WC}^{th}$ ,  $N_{OG}$  NEEDED TO OBTAIN  $PLP \leq 1E-4$  AS IN THE CASE  $N = 20$ ,  $N_C = 24$ ,  $p = 0.3$  FOR DIFFERENT  $(F, M)$ .

		$(F, M)$				
		(1, 24)	(2, 12)	(4, 6)	(6, 4)	(8, 3)
A	$\alpha^{th}$	0.6	0.25	0.0875	0.041667	0.025
	$N_{WC}^{th}$	288	120	42	20	12
	$N_{OG}$	21120	28800	45120	62400	80640
S	$\alpha^{th}$	0.65	0.3	0.125	0.06667	0.04375
	$N_{WC}^{th}$	312	144	60	32	21
	$N_{OG}$	22080	30720	48000	65280	83520

TABLE II

VALUES OF  $\alpha^{th}$ ,  $N_{WC}^{th}$ ,  $N_{OG}$  NEEDED TO OBTAIN  $PLP \leq 1E-6$  AS IN THE CASE  $N = 20$ ,  $N_C = 24$ ,  $p = 0.3$  FOR DIFFERENT  $(F, M)$ .

how the total number of WCs can be reduced substantially by increasing  $F$ . As an example, in Table I with  $F = 4$  using simulation,  $\alpha = 0.075$ , so the WC saving is equal to 92.5% with respect to a switch equipped with one WC per channel. In particular, every time  $F$  doubles,  $N_{WC}^{th}$  is reduced by more than half. The price to pay to obtain this saving in WC is the increase of the number of OGs, which increases almost linearly with the number of fibers  $F$ , and the increase is comprised between 50%-75% every time  $F$  doubles. The number of OGs evaluated with simulation and analysis do not differ much, in fact when  $F$  increases most of the complexity is related to the direct interconnection

of the input/output fibers, less to the connection of WCs. A trade-off among the number of WCs employed and the number of OGs need to be evaluated, thus choosing the proper value of  $F$ . Further evaluations and comparisons with other switch architectures with wavelength converters can be straightforwardly obtained by applying formulas, similar to (1), reported, for example, in [10].

## V. CONCLUSIONS

This paper presents an analytical model to evaluate packet loss in a shared per wavelength optical switch with multi-fiber interfaces. Besides filling a methodological gap regarding this kind of architecture and validating the analytical approach against simulation, the paper produces useful numerical results regarding the wavelength converters saving achieved by the approach with asynchronous operation. The switch design process shall take into account also component availability and cost to achieve an overall switch cost optimization, including both wavelength converters and space switching subsystems.

## REFERENCES

- [1] S. J. Ben Yoo, "Optical packet and burst switching technologies for the future photonic Internet", *IEEE J. Lightwave Technol.*, Vol. 24, pp. 4468-4492, Dec. 2006.
- [2] M. J. OMahony, C. Politi, D. Klonidis, R. Nejabati, D. Simeonidou, "Future Optical Networks", *IEEE J. Lightwave Technol.*, Vol. 24, Issue 12, pp. 4684-4696, Dec. 2006.
- [3] K. Vlachos, C. Raffaelli, S. Aleksic, N. Andriolli, D. Apostolopoulos, H. Avramopoulos, D. Erasme, E. Klonidis, M. N. Petersen, M. Scaffardi, K. Schulze, M. Spiropoulou, S. Sygletos, I. Tomkos, C. Vazquez, O. Zouraraki, F. Neri, "Photonics in switching: enabling technologies and subsystem design", *OSA J. Opt. Netw.*, Vol. 8, No. 5, pp. 404-428, May 2009.
- [4] S. Yao, B. Mukherjee, S. J. Ben Yoo, S. Dixit, "A Unified Study of Contention-Resolution Schemes in Optical Packet-Switched Networks", *IEEE J. Lightwave Technol.*, Vol. 21, pp. 672-683, 2003.
- [5] N. Akar, C. Raffaelli, M. Savi, E. Karasan, "Shared-per-wavelength asynchronous optical packet switching: A comparative analysis", *Computer Networks*, vol. 54, no. 13, pp. 2166-2181, 2010.
- [6] Y. Fukushima, H. Harai, S. Arakawa, M. Murata, "Design of Wavelength-convertible Edge Nodes in Wavelength-routed Networks", *J. Opt. Netw.*, Vol.5, No.3, pp.196-209, 2006.
- [7] C. Raffaelli, M. Savi, A. Stavdas, "Multistage Shared-per-Wavelength Optical Packet Switch: Heuristic Scheduling Algorithm and Performance", *IEEE J. Lightwave Technol.*, Vol. 27, Issue 5, pp. 538-551, March 2009.
- [8] C. Raffaelli, M. Savi, G. Tartarini, D. Visani, "Physical Path Analysis in Photonic Switches with Shared Wavelength Converters", in proceedings of ICTON 2010, Munich, Germany, June 27-July 1 2010, Mo.C1.5.
- [9] C. Raffaelli, M. Savi, "Power Consumption in Photonic Switches with Shared Wavelength Converters", in proceedings of ICTON 2010, Munich, Germany, June 27-July 1 2010, We.B1.6.
- [10] V. Eramo, A. Germoni, C. Raffaelli, M. Savi, "Multifiber Shared-Per-Wavelength All-Optical Switching: Architecture, Control and Performance", *IEEE J. Lightwave Technol.*, Vol. 26, Issue 5, pp. 537-551, March 2008.
- [11] C. Raffaelli, G. Mureto, "Combining Contention Resolution Schemes in WDM Optical Packet Switches with Multifiber Interfaces", *OSA Journal of Optical Networking*, special issue on Photonics in Switching, Vol. 6, N. 1, January 2007, page. 74-89, USA.
- [12] V. Eramo, A. Germoni, A. Cianfrani, M. Listanti, C. Raffaelli, "Evaluation of Power Consumption in Low Spatial Complexity Optical Switching Fabrics", *IEEE Journal of Selected Topics in Quantum Electronics*, 2010.